Oncogene (2020) 39:664–676
https://doi.org/10.1038/s41388-019-1014-0

ARTICLE

ITGB4-mediated metabolic reprogramming of cancer-associated fibroblasts

Jin Sol Sung[1] · Chan Woo Kang[1] · Suki Kang[2,3] · Yeonsue Jang[2] · Young Chan Chae[4] · Baek Gil Kim[1,2] · Nam Hoon Cho[1,2,3,5]

Received: 26 March 2019 / Revised: 28 August 2019 / Accepted: 5 September 2019 / Published online: 18 September 2019

Abstract

Integrin beta 4 (ITGB4) overexpression in cancer cells contributes to cancer progression. However, the role of stromal ITGB4 expression in cancer progression remains poorly understood, despite stromal ITGB4 overexpression in malignant cancers. In our study, ITGB4-overexpressing triple negative breast cancer (TNBC) cells provided cancer-associated fibroblasts (CAFs) with ITGB4 proteins via exosomes, which induced BNIP3L-dependent mitophagy and lactate production in CAFs. In coculture assays, the ITGB4-induced mitophagy and glycolysis were suppressed in CAFs by knocking down ITGB4 or inhibiting exosome generation in MDA-MB-231, or blocking c-Jun or AMPK phosphorylation in CAFs. ITGB4-overexpressing CAF-conditioned medium promoted the proliferation, epithelial-to-mesenchymal transition, and invasion of breast cancer cells. In a co-transplant mouse model, MDA-MB-231 made a bigger tumor mass with CAFs than ITGB4 knockdown MDA-MB-231. Herein, we presented how TNBC-derived ITGB4 protein triggers glycolysis in CAFs via BNIP3L-dependent mitophagy and suggested the possibility that ITGB4-induced mitophagy could be targeted as a cancer therapy.

Introduction

Tumor stromal metabolic support is an inevitable part in tumor progression. Recent cancer metabolism studies have shown that aerobic glycolysis in cancer-associated fibroblasts (CAFs), known as the reverse Warburg effect, is one such form of metabolic support. However, its mechanisms are largely unknown despite its importance in cancer research and therapy.

Cancer evolutionarily develops a variety of essential strategies for survival and progression including metabolic rewiring. For rapid proliferation, cancer cells require a large amount of energy for nucleotide, amino acid, and lipid precursor synthesis. However, in the overpopulated and restricted tumor microenvironment (TME), cancer cells are deprived of oxygen and nutrients due to poor vascularization [1]. To overcome these harsh environmental limitations, cancer cells reprogram the surrounding stromal cells including CAFs, to provide them with high-energy metabolites via aerobic glycolysis. Pavlides et al. reported that cancer cells induce aerobic glycolysis in neighboring stromal fibroblasts and take up the resulting products such as lactate and pyruvate for proliferation [2]. Although the reverse Warburg effect has not been completely elucidated, it is associated with cancer aggressiveness and poor outcomes. A promoted stromal glycolysis was observed during the progression from in situ to invasive breast cancer [3, 4] and significantly correlated with a poor prognosis in melanoma patients [5]. Due to its correlation with poor clinical

These authors contributed equally: Baek Gil Kim, Nam Hoon Cho

Supplementary information The online version of this article (https://doi.org/10.1038/s41388-019-1014-0) contains supplementary material, which is available to authorized users.

✉ Baek Gil Kim
bbaekiri@yuhs.ac

✉ Nam Hoon Cho
cho1988@yuhs.ac

[1] Brain Korea 21 Plus Project for Medical Science, Yonsei University College of Medicine, Seoul, South Korea

[2] Department of Pathology, Yonsei University College of Medicine, Seoul, South Korea

[3] Severance Biomedical Science Institute (SBSI), Yonsei University College of Medicine, Seoul, South Korea

[4] School of Life Sciences, Ulsan National Institute of Science and Technology, Ulsan, South Korea

[5] Global 5-5-10 System Biology, Yonsei University, Seoul, South Korea

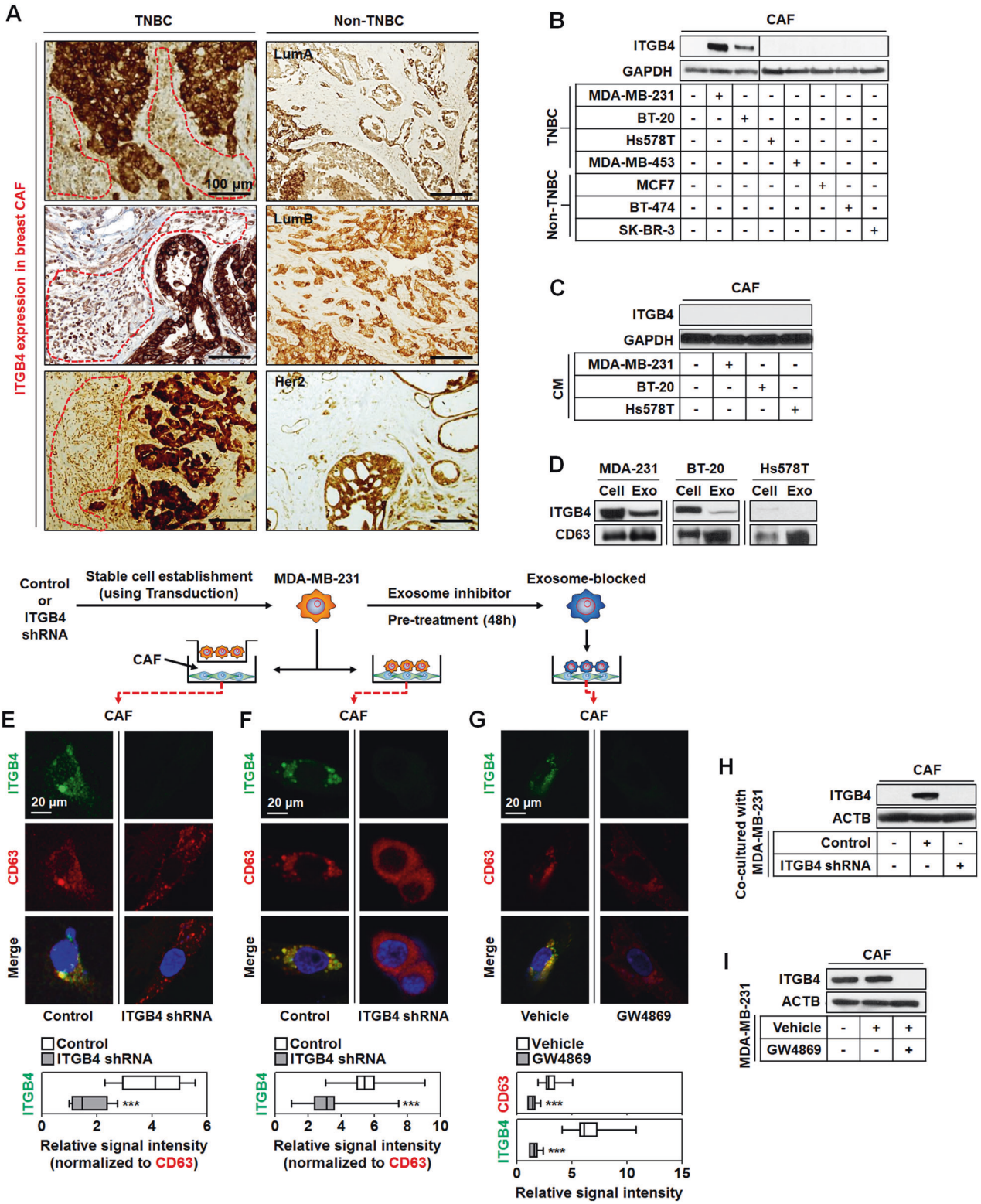

outcomes, the reverse Warburg effect is currently being considered as an anticancer therapeutic target [6]. A well-studied mechanism that triggers the reverse Warburg effect is reactive oxygen species (ROS)-induced mitophagy in CAFs. Martinez-Outschoorn et al. showed that cancer cells triggered oxidative stress-induced mitophagy in neighboring fibroblasts by secreting hydrogen peroxide, thereby facilitating stromal aerobic glycolysis [7]. As multiple

◀ **Fig. 1** ITGB4-overexpressing TNBC cells increased an ITGB4 protein level in cancer-associated fibroblasts via exosomal transfer. ITGB4 overexpression in **a** TNBC stroma and **b** CAFs cocultured with TNBC cells. TNBC ($n = 3$) and non-TNBC ($n = 9$; three luminal A, three luminal B, and three Her2) patient tissues were analyzed. A representative image was shown for each non-TNBC subtype. For coculture, the CAFs cultured on a plate were pre-stained with CellTracker Green CMFDA (5-chloromethylfluroecein diacetate). Next, unstained cancer cells were seeded onto the CMFDA-stained CAFs and cultured in serum-reduced DMEM/F12 (0.5% FBS) for 1 day. After coculture, the CMFDA-stained CAFs were separated from cancer cells using FACS sorter. **c** ITGB4 expression in CAFs stimulated with CMs from breast cancer cells. **d** ITGB4 expression in TNBC cells and -derived exosomes. TNBC-derived ITGB4 transfer to CAFs in **e** a transwell coculture and **f** a direct coculture. The signal intensity of ITGB4 was normalized to that of CD63. **g** Exosome-mediated ITGB4 transfer in the direct coculture. MDA-MB-231 cells were pretreated with 10 μM of GW4869 for 48 h. Statistical significance was determined using *t*-test. The expression levels of ITGB4 protein in **h** the CAFs directly cocultured with control or ITGB4 knockdown MDA-MB-231 cells and **i** the CAFs directly cocultured with the MDA-MB-231 cells treated with or without GW4869. CAFs were separated from direct coculture using FACS sorting. To establish stable ITGB4 knockdown cancer cells, MDA-MB-231 cells were transduced with the lentivirus containing control (empty) or ITGB4 shRNA. To block the exosomal transfer of ITGB4, MDA-MB-231 cells were pretreated with GW4869 for 1 day

forms of cellular stress are known to activate mitophagy in addition to ROS [8], it is necessary to investigate mitophagy-dependent aerobic glycolysis in CAFs to gain a better understanding of cancer metabolism. Previously, we found that breast fibroblasts such as CAFs do not express integrin beta 4 (ITGB4), however, were able to express ITGB4 through contact with triple negative breast cancer (TNBC) cells. ITGB4 neoexpression was induced in the primary CAFs cocultured with MDA-MB-231 cells [9]. Furthermore, integrins have been shown to regulate metabolic signaling pathways, for example ITGB1 triggered the TWIST-induced reprogramming of glucose metabolism in breast cancer [10]. As a result of these previous findings, we hypothesized that TNBC may facilitate the reverse Warburg effect by inducing ITGB4 expression in CAFs.

Results

ITGB4-overexpressing TNBC cells increased an ITGB4 protein level in CAFs via exosomal transfer

Previously, we found that MDA-MB-231 (a TNBC cell line), but not MCF7 (a non-TNBC cell line) cells, induced ITGB4 neoexpression in CAFs in a direct coculture system, suggesting that TNBC induces ITGB4 neoexpression in CAFs. As shown in Fig. 1a, ITGB4 was strongly expressed in TNBC stromal tissues, whereas it was rarely expressed in non-TNBC stromal tissues (luminal A, luminal B, and Her2 subtypes). To confirm this result, CAFs were cocultured with various TNBC and non-TNBC cells in a direct coculture system. ITGB4 expression was induced in CAFs by two TNBC cells, MDA-MB-231 and BT-20 (Fig. 1b). However, the TNBC cells, Hs578T and MDA-MB-453, and non-TNBC cells (MCF7: luminal B type, BT-474: luminal A type, SK-BR-3: Her2 type) were unable to induce ITGB4 expression in CAFs. Since ITGB4 expression can be induced by the soluble factors secreted from MDA-MB-231 and BT-20, CAFs were stimulated with the conditioned medium (CM) from MDA-MB-231, BT-20, and Hs578T (negative control) cells. However, ITGB4 expression was not induced by the CM from any of TNBC cells (Fig. 1c). Exosomes are an intercellular means of macromolecule exchange [11], therefore, we investigated whether ITGB4 was present in the exosomes of TNBC cells. As shown in Fig. 1d, ITGB4 was highly expressed in MDA-MB-231 and BT-20, and also detected in their exosomes. However, ITGB4 expression was not observed in Hs578T cells or their exosomes. The basal expression level of ITGB4 in breast cancer cells was shown in Supplementary Fig. S2. To further confirm that TNBC-derived exosomal ITGB4 protein was being transferred to CAFs, MDA-MB-231 cells showing the highest expression of ITGB4 were genetically manipulated to generate stable ITGB4 knockdown cells using shRNA lentiviral transduction (Supplementary Fig. S3), and then cultured with CAFs in a transwell or direct coculture system for 3 days. ITGB4 and CD63 (an exosome marker) were weakly co-localized in the CAFs cultured with MDA-MB-231 cells (control) in the transwell coculture system, however they were not co-localized in the CAFs cultured with ITGB4 knockdown MDA-MB-231 cells (Fig. 1e). Although CD63 was detected in the CAFs cocultured with ITGB4 knockdown MDA-MB-231 cells, ITGB4 expression was not detected. Similarly, in the transwell coculture system, ITGB4 and CD63 were strongly co-localized in the CAFs cultured with MDA-MB-231 cells (control), however they were not co-localized in the CAFs cultured with ITGB4 knockdown MDA-MB-231 cells (Fig. 1f). To further evaluate exosomal ITGB4 transfer, MDA-MB-231 cells were pretreated with GW4869 (10 μM, an exosome inhibitor) for 2 days, and then cultured with CAFs in a direct coculture system. As shown in Fig. 1g, the co-expression of ITGB4 and CD63 was dramatically reduced in the CAFs cultured with GW4869-treated MDA-MB-231 cells. ITGB4 protein expression was strongly detected in the CAFs cocultured with MDA-MB-231 cells, but not in those cocultured with ITGB4 knockdown MDA-MB-231 cells (Fig. 1h) and GW4869-treated MDA-MB-231 cells (Fig. 1i).

ITGB4 overexpression increased glycolysis in CAFs

A known role of CAFs in cancer progression is to produce high-energy metabolites via aerobic glycolysis, in a process called the reverse Warburg effect [2]. Therefore, we

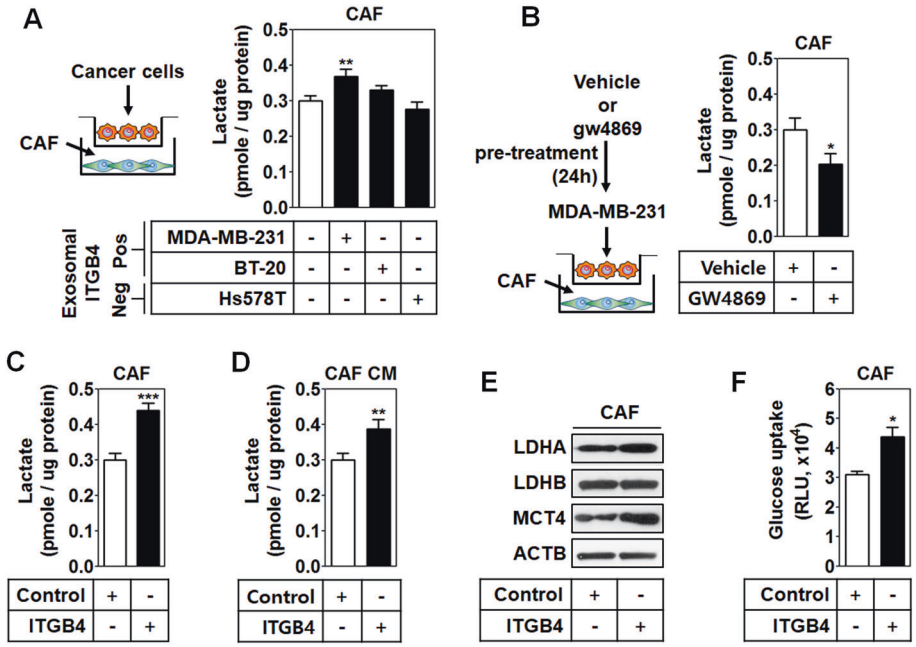

Fig. 2 ITGB4 overexpression increased glycolysis in cancer-associated fibroblasts. Lactate production in **a** CAFs cocultured with TNBC cells, **b** CAFs cocultured with GW4869-pretreated MDA-MB-231 cells, **c** CAFs transfected with ITGB4 plasmids, and **d** CM from ITGB4-overexpressing CAFs. The expression of the reverse Warburg effect-related proteins in **e** ITGB4-overexpressing CAFs. **f** Glucose uptake in ITGB4-overexpressing CAFs. Coculture was performed in the transwell coculture. The membrane pore size of transwell insert was 0.4 μm. Statistical significance was determined using *t*-test

investigated whether TNBC-derived exosomal ITGB4 transfer could increase the production of lactate, an end product of aerobic glycolysis, in CAFs. In a transwell coculture system, MDA-MB-231 significantly increased lactate production of CAFs (Fig. 2a), however the effect was inhibited by pretreatment with GW4869, an exosome inhibitor (Fig. 2b). To confirm that the increased glycolysis in CAFs was dependent on ITGB4 expression, we measured the amount of lactate in the cell lysate and CM of CAFs transfected with ITGB4 plasmids. The overexpression of ITGB4 was confirmed using both real-time PCR and western blot analyses (Supplementary Fig. S4). Lactate production was significantly increased by ITGB4 expression in both lysate (Fig. 2c) and in CM (Fig. 2d) of CAFs. In previous studies, the reverse Warburg effect has been defined as the conversion of pyruvate to lactate in CAFs and the export of lactate into the environment [2]. Therefore, we investigated the expression of lactate dehydrogenases and monocarboxylate transporter 4 (MCT4). As shown in Fig. 2e, the expression of dehydrogenase A (LDHA) and MCT4 was increased in CAFs by ITGB4 overexpression. Since glucose uptake can indicate increased glycolysis [12], glucose uptake was analyzed and was found to be increased in ITGB4-overexpressing CAFs (Fig. 2f).

ITGB4-dependent glycolysis was associated with mitochondrial fission and clearance

Aerobic glycolysis is associated with mitochondrial dynamics [13]. Thus, we compared the mitochondrial morphology of CAFs and ITGB4-overexpressing CAFs. Mitochondrial fission was increased in ITGB4-overexpressing CAFs compared with the control (Fig. 3a). In addition, ITGB4 overexpression promoted the expression of mitochondrial fission 1 protein (FIS1) and the phosphorylation (Ser616) of dynamin-1-like protein (DRP1) in CAFs (Fig. 3b), while it suppressed the expression of mitochondrial fusion-related proteins, mitochondrial dynamin like ATPase (OPA1) and mitofusin 1 (MFN1) (Fig. 3c). Mitophagy is essential for glycolytic switching [14]. Therefore, we examined whether ITGB4 overexpression was associated with mitophagy in CAFs. As shown in Fig. 3d, the mitochondria enclosed within double-membraned autophagosome was increased in ITGB4-overexpressing CAFs compared with the control. Mitochondria can activate both cell death and mitophagy in response to the same conditions [15]. So, we compared apoptosis between CAFs and ITGB4-overexpressing CAFs. However, there was no difference in apoptosis between CAFs and ITGB4-overexpressing CAFs (Fig. 3e).

ITGB4 overexpression induced BCL2 interacting protein 3 like (BNIP3L)-dependent mitophagy in CAFs

To investigate the ITGB4-induced mitophagy pathway, the expression of mitophagy-inducing factors was examined in ITGB4-overexpressing CAFs. As shown in Fig. 4a, the expression of BNIP3L showed a positive correlation with ITGB4 expression, whereas PTEN induced kinase 1 (PINK1) was barely affected by ITGB4 expression and parkin RBR E3 ubiquitin protein ligase (PRKN) was decreased. BCL2 Interacting Protein 3 (BNIP3) was not detected in CAFs or in ITGB4-overexpressing CAFs. The

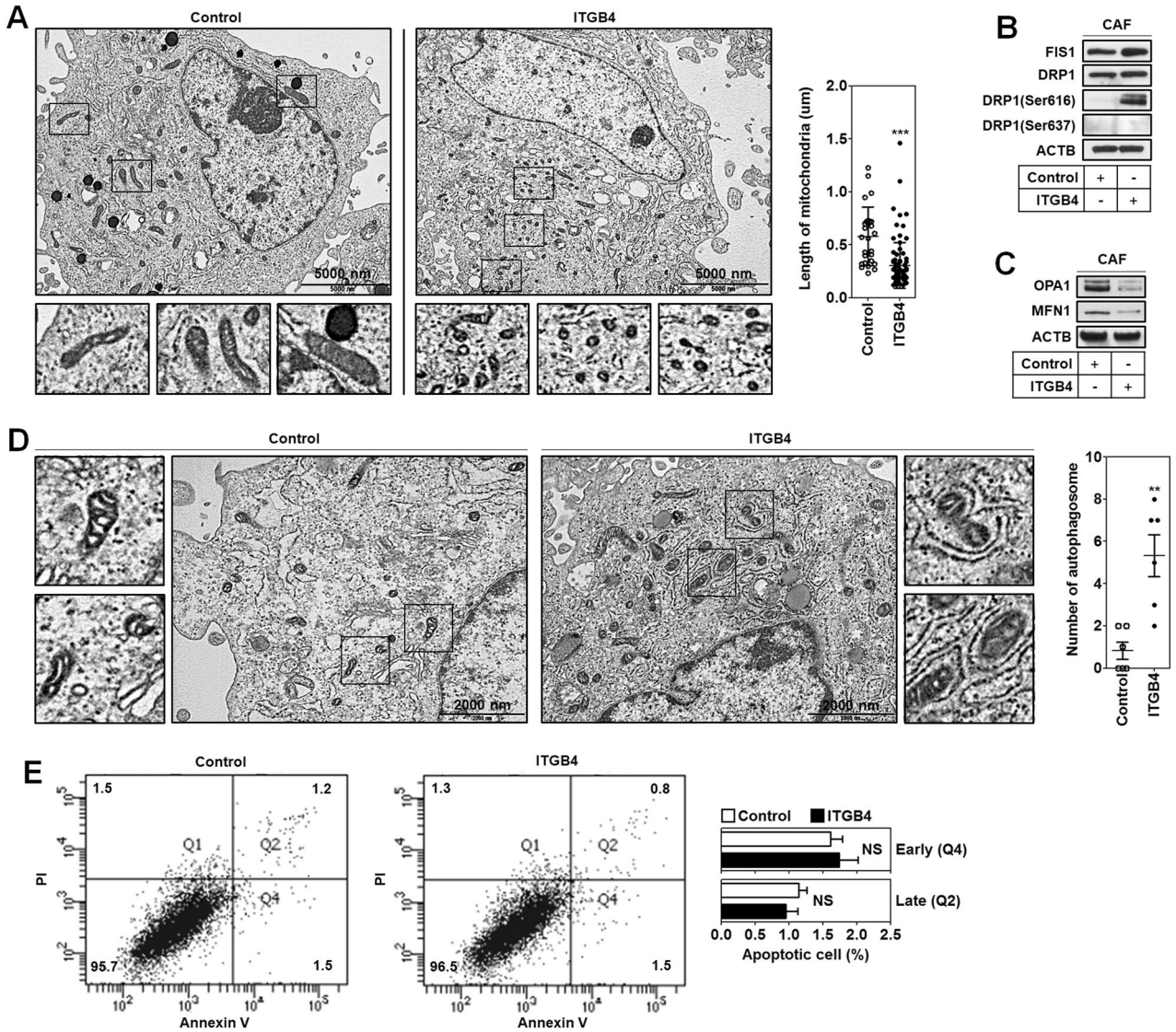

Fig. 3 ITGB4-dependent glycolysis was associated with mitochondrial fission and clearance. **a** The transmission electron microscopic image of ITGB4-induced mitochondrial fission. The length of mitochondria in electron microscopic images was measured using Image J. The expression of mitochondrial **b** fission and **c** fusion-related proteins. **d** The transmission electron microscopic image of ITGB4-induced mitochondrial clearance. **e** Cell viability comparison between wild-type and ITGB4-overexpressing CAFs. A representative one of three independent experiments. Statistical significance was determined using *t*-test

ITGB4-dependent expression of BNIP3L was further validated by in situ fluorescence analysis. BNIP3L was co-localized with ITGB4 on ITGB4-overexpressing CAFs (Fig. 4b), suggesting that ITGB4 regulates BNIP3L expression in CAFs. Therefore, we analyzed the 2 kb upstream sequence of BNIP3L gene to find potential transcription factor binding sites, especially for integrin-activating and glycolysis-related transcription factors. Three putative c-Jun binding sites were predicted. According to previous reports, integrins mediate c-Jun activation [16] and c-Jun N-terminal kinase 2 is essential for Ras-induced glycolysis [17]. Three 500-bp-sized wild-type promoter sequences (S1W, S2W, and S3W) were amplified from the genomic DNA of CAFs using conventional PCR. Binding site deletion mutants (S1D, S2D, and S3D) were constructed from the wild-type PCR products by an overlap extension PCR method. The wild-type and deletion mutant constructs were cloned into a pGL3 vector. To confirm that c-Jun bound to these sites, a dual-luciferase reporter assay was performed using plasmids containing a wild-type or mutant sequence (Supplementary Fig. S5). Luciferase activity was significantly reduced in the site 1 (S1D: −1995 to −1988) and 3 (S3D: −99 to −92) deletion mutants but not in the site 2 (S2D: −718 to −711) mutant compared with their wild types (Fig. 4c). Furthermore, ITGB4 overexpression increased c-Jun phosphorylation and

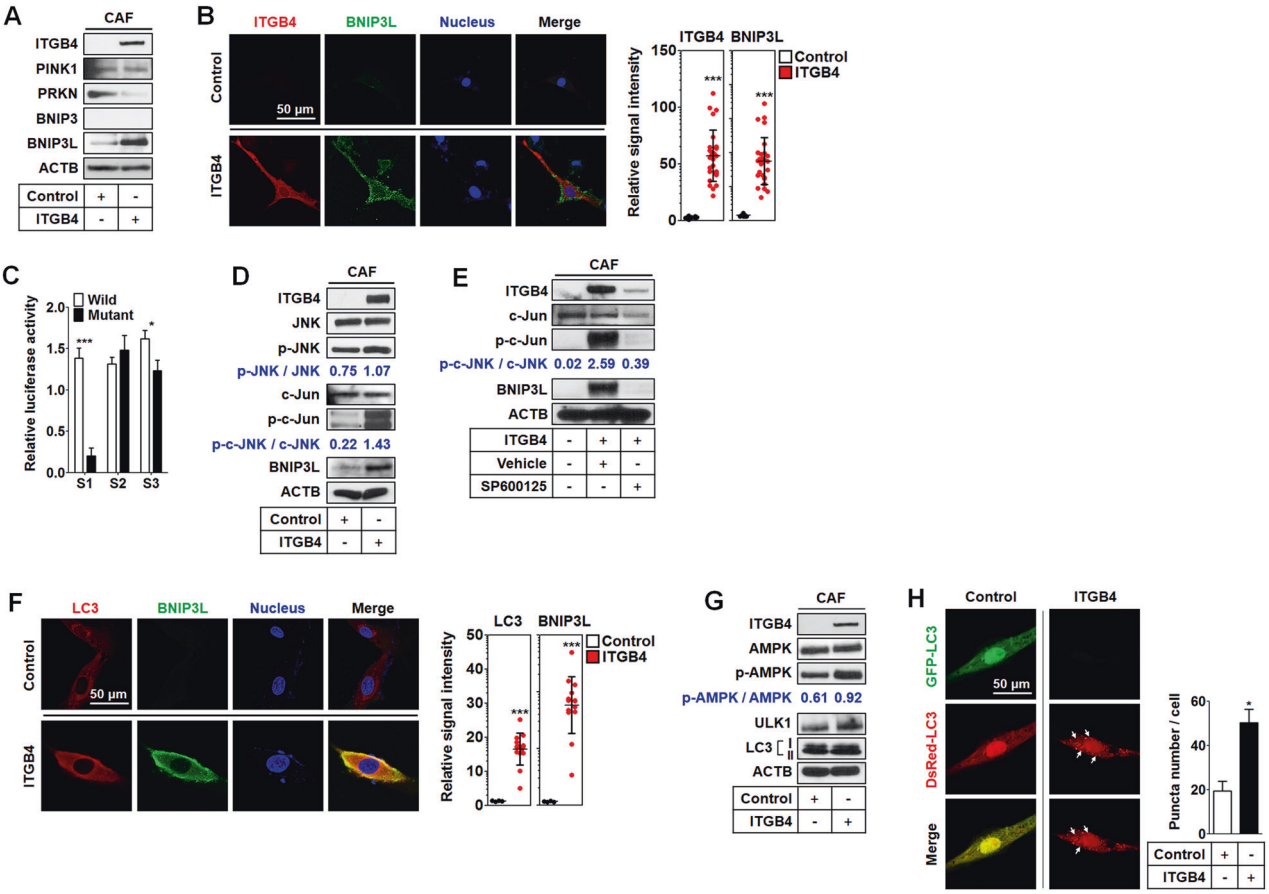

Fig. 4 ITGB4 overexpression induced BNIP3L-dependent mitophagy in cancer-associated fibroblasts. **a** The expression of mitophagy-related factors in the ITGB4-overexpressing CAFs. **b** The fluorescent microscopic image of ITGB4-induced BNIP3L overexpression in CAFs. **c** Dual-luciferase reporter assay. The putative c-Jun binding sites in the 2 kb upstream sequences of human BNIP3L gene were analyzed using PROMO. Three 500-bp-sized wild-type promoter sequences (S1W, S2W, and S3W) were amplified from the genomic DNA of CAFs using conventional PCR. Binding site deletion mutants (S1D, S2D, and S3D) were constructed from the wild-type PCR products by an overlap extension PCR method. The wild-type and deletion mutant constructs were cloned into a pGL3 vector. c-Jun binding to BNIP3L was examined by dual-luciferase assay. **d** ITGB4-dependent mitophagy signaling pathway in CAFs. **e** The suppression of ITGB4-dependent mitophagy signaling in CAFs by JNK inhibitor. **f** Co-expression between LC3 and BNIP3L in ITGB4-overexpressing CAFs. **g** ITGB4-induced autophagy signaling in CAFs. **h** Puncta formation in ITGB4-overexpressing CAFs. For a puncta formation assay, pQCXI Puro DsRed-LC3-GFP was transfected into CAFs, $n = 5$ for each group. Statistical significance was determined using *t*-test

BNIP3L expression in CAFs (Fig. 4d). The c-Jun-dependent expression of BNIP3L was further validated by treating ITGB4-overexpressing CAFs with SP600125 (20 μM), a JNK inhibitor, for 24 h. As shown in Fig. 4e, SP600125 inhibited both c-Jun phosphorylation and BNIP3L expression. BNIP3L forms autophagosomes with microtubule associated protein 1 light chain 3 (LC3) [18, 19]. Therefore, we examined the co-expression of BNIP3L and LC3, which was clearly observed in ITGB4-overexpressing CAFs (Fig. 4f). Autophagy is mediated by AMP-activated protein kinase (AMPK) via unc-51 like autophagy activating kinase 1 (ULK1) [20]. ITGB4 overexpression increased AMPK phosphorylation and ULK1 expression in CAFs (Fig. 4g). To further confirm ITGB4-induced autophagosome formation, we performed a puncta formation assay using the DsRed-LC3B-GFP reporter, which GFP is degraded by Cys-protease ATG4A from the reporter once autophagy begins [21]. As shown in Fig. 4h, the GFP signal decreased and the number of puncta increased in ITGB4-overexpressing CAFs.

ITGB4-dependent reverse Warburg effect contributes to breast cancer progression

To investigate whether ITGB4-induced mitophagy in CAFs contributes to TNBC progression via the reverse Warburg effect, MDA-MB-231 cells were treated with the CM from control CAFs, ITGB4-overexpressing CAFs, or ITGB4-overexpressing CAFs pretreated with compound C (10 μM), an AMPK inhibitor. The proliferation of MDA-MB-231 cells was significantly increased by the CM from ITGB4-overexpressing CAFs compared with the control (Fig. 5a), and was suppressed by AMPK inhibition in ITGB4-

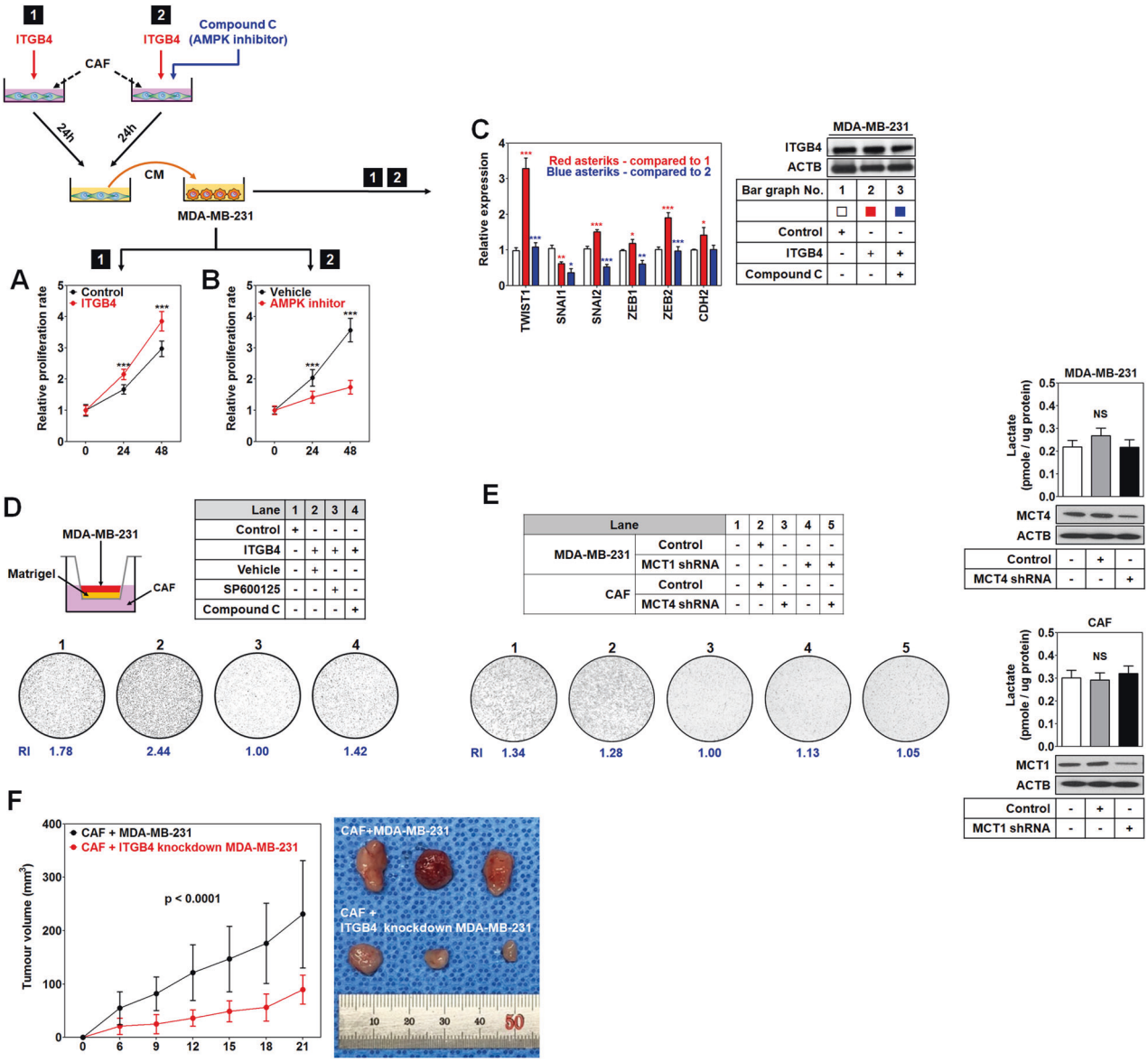

Fig. 5 ITGB4-dependent reverse Warburg effect contributes to breast cancer progression. The proliferation of TNBC cells stimulated by CM from **a** ITGB4-overexpressing CAFs and **b** ITGB4-overexpressing CAFs pretreated with compound C (AMPK inhibitor, 10 μM, pretreatment for 24 h). **c** The upregulation of EMT inducers in TNBC cells by ITGB4-overexpressing CAFs. EMT inducer expression was analyzed using real-time PCR. MDA-MB-231 cells were stimulated with CM from CAFs transfected with control or ITGB4 plasmids. Compound C was pretreated to inhibit ITGB4-induced mitophagy in CAFs. **d** Increased cancer invasiveness by ITGB4-induced mitophagy in CAFs. CAFs and MDA-MB-231 cells were seeded to lower chamber and matrigel-coated transwell insert, respectively, The invaded cells to the lower surface of the matrigel were stained with 0.1% crystal violet. **e** Increased cancer invasiveness by the uptake of CAF-derived lactates. MDA-MB-231 cells and CAFs were transfected with MCT1 and MCT4 shRNA, respectively. **f** Increased cancer growth by ITGB4 knockdown CAFs in a mouse xenograft model. MDA-MB-231 or ITGB4 knockdown MDA-MB-231 cells were subcutaneously co-transplanted with CAFs. Statistical significance was determined using *t*-test

overexpressing CAFs (Fig. 5b). Lactate availability is associated with the epithelial-mesenchymal transition (EMT) in cancer cells [22]. Therefore, the expression of EMT inducers and CDH2, which represent the EMT phenotype, was examined in MDA-MB-231 cells stimulated with CMs. Twist family BHLH transcription factor 1, snail family transcriptional repressor 2, zinc finger E-box binding homeobox 1 (ZEB1), ZEB2, and N-cadherin (CDH2) were upregulated in MDA-MB-231 cells treated with the CM from ITGB4-overexpressing CAFs compared with the control, and were suppressed by AMPK inhibition in ITGB4-overexpressing CAFs (Fig. 5c). To examine TNBC invasiveness alteration is associated with ITGB4-induced mitophagy in CAFs, an invasion assay was performed using the transwell coculture system. The invasion of MDA-MB-231 cells was increased by the coculture with ITGB4-

overexpressing CAFs compared with the control, but not by coculture with ITGB4-overexpressing CAFs pretreated with SP600125 and compound C (Fig. 5d). To validate that CAF-derived lactate contributes to the invasiveness of MDA-MB-231 cells, we performed invasion matrigel assay using MCT1-knockdown MDA-MB-231 and MCT4-knockdown CAFs. The knockdown of MCT1 and/or MCT4 did not induce a significant change in lactate production in cells but decreased the invasiveness of the MDA-MB-231 cells cocultured with CAFs (Fig. 5e). Next, to confirm the ITGB4-mediated metabolic reprogramming of CAFs by TNBC cells, wild-type and ITGB4 knockdown MDA-MB-231 cells were subcutaneously transplanted into BALB/c nude mice with immortalized CAFs. The growth of ITGB4 knockdown MDA-MB-231 cells was significantly reduced compared with the wild type (Fig. 5f). The viability of immortalized CAFs in vivo was confirmed by fluorescence microscopy after scarifying mice (Supplementary Fig. S6).

Discussion

Following on from our previous study, "TNBC cell-induced ITGB4 neoexpression in CAFs", we have demonstrated that ITGB4-overexpressing TNBC cells can provide CAFs with ITGB4 proteins via exosomal transfer. As cancer is a metabolic disease, it requires large amounts of energy to sustain uncontrolled cell growth. The rapid and unlimited proliferation of cancer cells can deplete energy resources within a restrictive tumor environment and threaten the survival of cancer cells themselves, thereby enforces them to develop ways of overcoming their environment. The reverse Warburg effect, aerobic glycolysis in CAFs, is a form of stromal metabolic reprogramming, which can be induced by cancer-derived stimuli to support cancer growth and progression by providing high-energy metabolites [2]. Therefore, we hypothesized that exosomal ITGB4 transfer triggers the reverse Warburg effect in TNBC. Integrin-mediated glycolysis seemed to be unfamiliar as no studies have yet reported. However, our assumption was partly supported by a previous study performed by Yang et al., who demonstrated the ITGB1-induced reprogramming of glucose metabolism in breast cancer [10]. Interestingly, laminin-332, a unique ITGB4 ligand, is not only overexpressed in CAFs stimulated by TNBC cells [9] but also in the fibrotic stroma neighboring invasive breast cancer [23]. Considering that a laminin-332-rich TME is naturally established around TNBC and that ITGA6 (the only pair partner) is intrinsically expressed at a high level in CAFs (Supplementary Fig. S7), the exosomal ITGB4 transfer to CAFs may be an adaptation of TNBC to its microenvironment in order to increase its probability of survival. In addition to glycolysis, the exosomal ITGB4 transfer to CAFs is likely to contribute to angiogenesis. Previously, we showed that tumor growth-generated compressive stress promoted a signaling axis for VEGFA production in CAFs by inducing the overexpression of LAMC2, ITGA6, and EIF4E [24]. The exosomal transfer of ITGB4 to CAFs may complete the VEGFA signaling pathway by paring with ITGA6.

ITGB4-dependent mitophagy appears to be a potential mechanism of metabolic rewiring in cancer. Mitophagy, a well-studied mechanism that triggers aerobic glycolysis, is generally induced by ROS and hypoxia in cancers. Cancer cells generate more ROS than normal cells [25], which increases mitochondrial dysfunction [26] and a subsequent mitophagy [15]. Ironically, ROS are a double-edged sword for cancer as they can facilitate cancer progression at low levels, yet suppress cancer at high levels by inhibiting growth and inducing cell death [27, 28]. Mitophagy is also triggered by low levels of ROS. Frank et al. reported that a mild ROS induces mitophagy in a mitochondrial fission dependent manner [29]. Since the levels of ROS are elevated during tumor growth [30], ROS-dependent mitophagy may not occur during the later stages of tumor progression. Unlike ROS, the increased expression of ITGB4 is beneficial for cancer and stromal cells. The well-known functions of ITGB4 are to promote cancer growth [31] and anoikis resistance in CAFs [9]. Hypoxia is also induced by cancer growth as it occurs in tissue with a low oxygen concentration [32], thereby triggers HIF1-induced mitophagy [33]. This may mean that hypoxic conditions are weak or not maintained in the fibrotic stroma surrounding a tumor for relatively high oxygen availability. Thus, ITGB4-dependent mitophagy may be more suitable for the fibrotic tumor stroma. As shown in Fig. 1a, ITGB4 is overexpressed in the stroma neighboring a tumor mass in TNBC tissue. This stromal tissue is at a distance from the tumor and is therefore unlikely to be hypoxic. Interestingly, ITGB4 triggers mitophagy in a BNIP3L-dependent manner unlike ROS and hypoxia, which generally use the PINK1-Parkin and BNIP3 pathways for mitophagy, respectively [33, 34].

Metabolic rewiring is associated with a poor prognosis in cancer, and has, therefore, grabbed the attention of cancer researchers and clinicians. In this study, we presented a novel mechanism in which TNBC-derived ITGB4 triggers aerobic glycolysis in CAFs via BNIP3L-dependent mitophagy (Fig. 6). We also suggested the possibility that ITGB4-induced mitophagy could be targeted as a cancer therapy by blocking various parts of the mechanism such as the release of exosomes from TNBC, ITGB4-induced JNK activation, and AMPK-mediated mitophagy in CAFs. Among them, JNK inactivation may be the best of these options as cumulative studies have reported that JNK inhibitors could be used in the therapy of various cancers

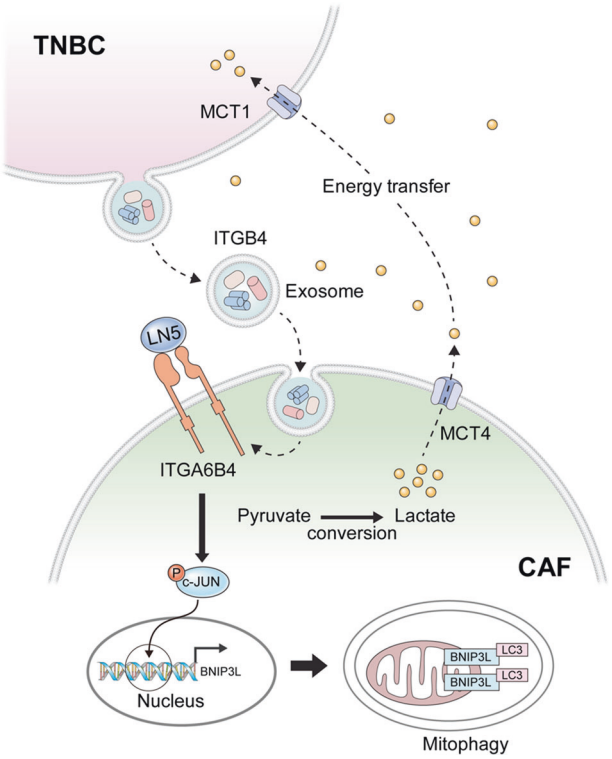

Fig. 6 ITGB4-mediated metabolic reprogramming of cancer-associated fibroblasts in breast cancer. ITGB4-overexpressing TNBC cells provide CAFs with ITGB4 via exosomes. Once ITGB4 is transferred, integrin α6β4 is displayed on the surface of CAFs. LN5 (laminin-332) in extracellular microenvironment binds to the integrin α6β4, and then initiates the mitochondrial expression of BNIP3L in CAFs via c-Jun phosphorylation. BNIP3L triggers mitophagy by binding with LC3, which results in the conversion of pyruvate to lactate in the CAFs. The produced lactates are exported from CAFs to extracellular microenvironment through MCT4, and then TNBC cells uptake them through MCT1

[35]. However, the inhibition of ITGB4 and exosome release should not be dismissed. Liu et al. reported that the small chiral molecule, SEC, selectively promotes apoptosis in ITGB4-expressing cancer cells by inducing the nuclear translocation of ITGB4 [36], while Kosgadage et al. showed that the anticancer effects of cannabidiol are partly due to its regulatory effects on exosome biogenesis [37]. Last but not least, this novel mechanism should be further investigated in other cancers since many intractable cancers including pancreatic cancer show ITGB4 overexpression.

Materials and methods

Human fibroblast isolation and cell cultures

CAFs were isolated from the breast cancer patients undergoing surgery at Severance Hospital of the Yonsei University Health System, South Korea. The research protocol was approved by the Severance Hospital Ethics Committee (IRB number 4-2008-0383). All patients were informed of tissue use of comprehensive experiments and signed consent forms. To isolate CAFs, tissue was cut into small pieces, placed in a digestion solution of enzyme cocktail (ISU ABXIS, Seoul, South Korea), and incubated in a humidified incubator at 37 °C and 5% CO_2 overnight. The digested cell mixture was filtered through a 70 µm cell strainer (BD Bioscience, Franklin Lakes, NJ) and then centrifuged at $485 \times g$ for 5 min. The resulting pellet was resuspended with medium, added into the Ficoll (Histopaque®-1077, sigma, 1.077 g/ml), and centrifuged at $90 \times g$ for 2 min. The supernatant containing fibroblasts was further centrifuged at $485 \times g$ for 9 min. The final pellet was resuspended with the Dulbecco's Modified Eagle Medium: Nutrient Mixture F12 (DMEM/F12, Gibco BRL, Grand Island, NY) containing 20% fetal bovine serum (FBS; Gibco BRL, Grand Island, NY) supplemented with 100 IU/ml penicillin, 100 µg/ml streptomycin (Gibco BRL, Grand Island, NY), and then placed in a humidified incubator containing 5% CO_2 at 37 °C. The fibroblastic characteristics of the isolated cells were determined by both microscopic morphology and immunostaining with antibodies against vimentin (VIM, ab-20346, Abcam, Cambridge, UK), alpha-smooth muscle actin (α-SMA, ab7817, Abcam, Cambridge, UK), and cytokeratin (CK, sc-32721, Santa Cruz Biotechnology, Dallas, TX) (Supplementary Fig. S1). Breast cancer cell lines (MDA-MB-231, BT-20, MDA-MB-453, MCF7, BT-474, and SK-BR-3 cells) were purchased from the Korean Cell Line Bank (authenticated using morphology and STR profiling) and cultured with the DMEM (Gibco BRL, Grand Island, NY) containing 10% FBS (Gibco BRL, Grand Island, NY) supplemented with 100 IU/ml penicillin, 100 µg/ml streptomycin (Gibco BRL, Grand Island, NY) under the same experimental conditions as the fibroblasts. For coculture, CAFs were incubated with the serum-free DMEM/F12 containing 5 µM CellTracker Green CMFDA (5-chloromethylfluroecein diacetate; Invitrogen, Carlsbad, CA) dye at 37 °C for 30 min, washed with phosphate buffered saline (PBS, Gibco BRL, Grand Island, NY), and added with a fresh medium. Unstained cancer cells were seeded onto the CMFDA-stained CAFs, and then cultured with serum-reduced DMEM/F12 (0.5% FBS) for 1 day. All the cells used in this study were confirmed to be mycoplasma-negative using MycoAlert® Mycoplasma Detection Kit (Lonza, Basel, Switzerland).

Real-time PCR analysis

Total RNA was extracted using TRIzol (Invitrogen, Carlsbad, CA) and quantitated by NanoDrop Spectrophotometer (ThermoFisher Scientific, Waltham, MA). For cDNA synthesis, 1 µg of total RNA was reverse-transcribed using

Hyperscript™ First strand synthesis kit (Geneall, Seoul, Korea) in a PTC-200 Thermal Cycler (MJ Research, Reno, NV, USA). For quantitative analysis, 25 ng of the resulting cDNA was amplified in a CFX Connect™ Real-Time PCR Detection System (Bio-Rad Laboratories; Hercules, CA, USA) using LaboPass™ SYBR Green Q Master (Cosmogenetech, Seoul, South Korea). The PCR experiments were performed in triplicated, and relative expression was normalized to endogenous glyceraldehyde-3-phosphate dehydrogenase (GAPDH) and calculated according to the ΔΔCt method. All primer sequences were provided in Supplemental Table S1.

Genetic manipulation

For a transient gene overexpression, CAFs were seeded into a six-well plate to reach 80% confluence. Before transfection, the CAFs were incubated in Opti-MEM for 2 h (Gibco BRL, Grand Island, NY). Plasmid vectors (empty, ITGA6, ITGB4, pQCXI Puro DsRed-LC3-GFP, MCT1 shRNA: MISSION® TRC TRCN0000038339, or MCT4 shRNA: MISSION® TRC TRCN0000038444) were transfected into MDA-MB-231 cells or CAFs using Lipofectamine® LTX with Plus™ overnight according to the manufacturer's manual and then incubated for 24 h. pQCXI Puro DsRed-LC3-GFP was a gift from David Sabatini (Addgene plasmid #31182; http://n2t.net/addgene:31182; RRID: Addgene_31182). To establish an ITGB4 knockdown MDA-MB-231 cells, MDA-MB-231 cells were transduced with lentivirus containing ITGB4 shRNA and selected with puromycin (Sigma-Aldrich Corporation, St. Louis, MO). Single-cell clones were obtained using limiting dilution and their knockdown of ITGB4 was confirmed by western blot.

Western blot analysis

Protein extracts were prepared by cell lysis with a PRO-PREP™ kit (iNtRON Biotechnology, Seongnam-si, South Korea) and centrifuged at 15,000 × *g* for 15 min using Centrifuge 5810R (Eppendorf, Hamburg, Germany). The protein concentration of the resulting supernatant was measured using the Bradford protein assay kit (Bio-Rad, Hercules, CA). Twenty micrograms protein was electrophoresed on 10% polyacrylamide gels in Tris/glycine (Invitrogen®, Carlsbad, CA), transferred to a polyvinylidene difluoride membrane (Millipore Corporation, Billerica, MA), and then probed with primary antibodies against LAMC2 (sc-28330), ITGA6 (sc-10730), ITGB4 (sc-9090), ACTB (sc-47778), GAPDH (sc-20357), CD63 (sc-15363), PINK1 (sc-33796), PRKN (sc-32282), BNIP3 (sc-56167), BNIP3L (sc-166332), JNK (sc-571), p-JNK (sc-6254), c-Jun (sc-1694), p-c-Jun (sc-822), FIS1 (sc-376469), MCT1 (sc-365501), MCT4 (sc-50329) (Santa Cruz Biotechnology, Dallas, TX), OPA1 (#80471), MFN1 (#14739), DRP1 (#8570), DRP1(Ser616, #3455), DRP1(Ser637, #4867) (Cell signaling technology, Danvers, MA), ULK1 (PA5-34542, Invitrogen, Carlsbad, CA), AMPK (ab32047), p-AMPK (ab133448), LDHA (ab-125683), LDHB (ab-75167), and LC3 (ab-48394) (Abcam; Cambridge, UK). The blotted membrane was blocked with 0.5% BSA at RT for 1 h and then followed by incubation with HRP-tagged secondary antibodies against mouse (SA001), rabbit (SA002) (GenDEPOT, Barker, TX), or goat (811620, Invitrogen, Carlsbad, CA). Immunoreactive bands were visualized by enhanced chemiluminescence detection kit (GenDEPOT, Barker, TX).

Lactate assay

The amount of lactate in cell lysate and supernatant was measured using Lactate assay kit (Biovision, Milpitas, CA) according to the manufacturer's instructions. Briefly, 50 µl of sample was mixed with 50 µl of the master reaction mix containing 46 µl of lactate assay buffer, 2 µl of lactate enzyme mix, and 2 µl of lactate probe in a well of a 96-well plate. Thirty minutes after incubation, absorbance was measured at 570 nm using Spectramax plus 96/384 (MTX Lab Systems, Bradenton, FL, USA). Lactate amount was measured in triplicate, calculated using the standard curve prepared with known concentration of lactate, and then normalized with protein concentration.

Transwell matrigel invasion assay

CAFs and MDA-MB-231 cells were seeded to lower chamber and matrigel-coated transwell insert respectively and then placed in a humidified incubator at 37 °C and 5% CO2 for 24 h. After incubation, non-invading cells were removed from the upper surface of the matrigel by scrubbing. The invaded cells to the lower surface of the matrigel were stained with 0.1% crystal violet and rinsed with distilled water. The dried matrigel was placed on a slide, added with a drop of immersion oil, and then covered with a coverslip.

Exosome isolation

CMs were collected from cancer cells and centrifuged at 3000 × *g* for 15 min. The resulting supernatant was transferred to a new tube, mixed with the appropriate volume of ExoQuick-TC (SBI, Palo Alto, CA), incubated at 4 °C for 24 h, and then centrifuged at 1500 × *g* for 30 min. The supernatant was aspirated and then the mixture was centrifuged at 1500 × *g* for 5 min to remove residual supernatant. The exosome pellet was resuspended to use or stored at −20 °C.

Apoptosis detection assay

Apoptosis was analyzed using Annexin V-FITC detection kit (BD Bioscience, Franklin Lakes, NJ) according to the manufacturer's instructions. Briefly, CAFs were washed twice with cold PBS, centrifuged, and then resuspended with binding buffer at a concentration of 1×10^6 cells/ml. One hundred microlitres of the cell suspension was mixed with 5 µl of Annexin V-FITC and PI and then incubated in the dark at room temperature for 15 min, the mixture was added with 400 µl of binding buffer and then analyzed using FACSVerse (BD Bioscience, Franklin Lakes, NJ).

Glucose uptake assay

Glucose uptake was measured using Glucose Uptake Glo kit (Promega, Madison, WI) according to the manufacturer's instructions. CAFs (1.5×10^4) were seeded in a well of 96-well plate and placed for 24 h. The CAFs were washed with glucose-free PBS and incubated with 2DG (1 mM) for 10 min. Stop and neutralization buffer were added to the well and mixed one by one. 2DG6P detection reagent was added to the CAFs and then incubated at RT for 30 min. Glucose uptake was measured using luminometer (EG & G Berthold, Bad Wildbad, Germany) in triplicate.

Xenograft mouse model

GFP-overexpressing CAFs (3×10^6) were subcutaneously co-transplanted to 6-week-old female BALB/c nude mice with RFP-overexpressing MDA-MB-231 or RFP-overexpressing ITGB4 knockdown MDA-MB-231 cells (1×10^6) using Matrigel (Invitrogen, Carlsbad, CA). Tumor size (length and width) was measured every 3 days using calipers for one month. The volume of tumor mass was calculated using the formula: $V = (W \times W \times L)$, where W is the width and L is the length. The research protocol was approved by Yonsei University Health System Institutional Animal Care and Use Committee (2016-0312).

Transmission electron microscopic analysis

CAFs transfected with control or ITGB4 plasmid were harvested with trypsin-EDTA (Gibco BRL, Grand Island, NY), placed to 1.5 ml tube, and immediately fixed with 4% paraformaldehyde at RT for 30 min. After washing three times with PBS by centrifugation at $300 \times g$ for 5 min, the CAFs were embedded in 100% Eponate resin (Ted Pella Inc, Redding, CA) at 60 °C for 24 h. One micrometer thick sections were cut using an ultramicrotome (Leica, Wetzlar, Germany), stained with 2% aqueous uranyl acetate for 15 min, rinsed with distilled water, and then stained with lead citrate (Leica, Wetzlar, Germany). The stained sections were examined on JEM1011 transmission electron microscope (JEOL, Tokyo, Japan).

Confocal imaging analysis

CAFs were fixed with 4% paraformaldehyde at 4 °C for 15 min and then permeabilized with 1% Triton X-100 (Sigma-Aldrich, St. Louis. Mo) at RT for 10 min. After being washed twice with PBST, the CAFs were blocked with 1% BSA at RT for 1 h and then incubated with primary antibodies against ITGB4 (sc-9090), CD63 (sc-15363), and BNIP3L (sc-166332) (Santa Cruz Biotechnology, Dallas, TX) LC3 (ab-48394) (Abcam; Cambridge, UK) at 4 °C overnight. Following washing, fluorescence-conjugated secondary antibodies against mouse (sc-2010) or rabbit (sc-2012, sc-3753) (Santa Cruz Biotechnology, Dallas, TX) were added to the CAFs and incubated at RT for 1 h. The CAFs were washed, added with a drop of mounting solution containing DAPI (Abcam, Cambridge, UK), covered with a coverslip, and then analyzed with LSM700 laser scanning confocal microscope (Carl Zeiss, Oberkochen, Germany).

Luciferase assay

The putative c-Jun binding sites were analyzed in the 2 kb upstream sequences of human *BNIP3L* gene using PROMO [38]. Three putative binding sites on *BNIP3L* were amplified from the genomic DNA of CAFs using conventional PCR. Deletion mutants were constructed from the PCR products by an overlap extension PCR method [39]. The wild-type and deletion mutant constructs were cloned into pGL3 vector. For dual-luciferase assays, each cloned plasmid was co-transfected with pRL-TK in HEK293T (2×10^5) cells using Lipofectamine® LTX with Plus™ Reagent (Invitrogen®, Carlsbad, CA, USA). Forty-eight hours after transfection, luciferase activity was measured from the cell lysates using a dual-luciferase reporter assay system (Promega; Madison, WI, USA) using luminometer (EG & G Berthold, Bad Wildbad, Germany).

Statistical analysis

Statistical significance was determined using *t*-test. The results were considered to be significant at $p < 0.05$ and presented with ±standard deviation. All statistical analyses were performed using Prism 6 for Windows (GraphPad Software, Inc.; La Jolla, CA). Asterisks indicate p values: one for $p < 0.05$, two for $p < 0.01$, and three for $p < 0.001$.

Acknowledgements This study was supported by the Mid-Career Researcher Program (no. 2019R1A2B5B01069934; NHC) and Challenges in Creative Research (no. 2019R1I1A1A01060549; BGK) through a National Research Foundation of Korea grant, and The Health Fellowship Foundation grants funded by Yuhan Corporation.

The authors thank Medical Illustration & Design, a part of the Medical Research Support Services of Yonsei University College of Medicine, for all artistic support related to this work.

Compliance with ethical standards

Conflict of interest The authors declare that they have no conflict of interest.

Publisher's note Springer Nature remains neutral with regard to jurisdictional claims in published maps and institutional affiliations.

References

1. Ratnikov BI, Scott DA, Osterman AL, Smith JW, Ronai ZA. Metabolic rewiring in melanoma. Oncogene. 2017;36:147–57.
2. Pavlides S, Whitaker-Menezes D, Castello-Cros R, Flomenberg N, Witkiewicz AK, Frank PG, et al. The reverse Warburg effect: aerobic glycolysis in cancer associated fibroblasts and the tumor stroma. Cell Cycle. 2009;8:3984–4001.
3. Martins D, Beca FF, Sousa B, Baltazar F, Paredes J, Schmitt F. Loss of caveolin-1 and gain of MCT4 expression in the tumor stroma: key events in the progression from an in situ to an invasive breast carcinoma. Cell Cycle. 2013;12:2684–90.
4. Witkiewicz AK, Dasgupta A, Nguyen KH, Liu C, Kovatich AJ, Schwartz GF, et al. Stromal caveolin-1 levels predict early DCIS progression to invasive breast cancer. Cancer Biol Ther. 2009;8:1071–9.
5. Wu KN, Queenan M, Brody JR, Potoczek M, Sotgia F, Lisanti MP, et al. Loss of stromal caveolin-1 expression in malignant melanoma metastases predicts poor survival. Cell Cycle. 2011;10:4250–5.
6. Fu Y, Liu S, Yin S, Niu W, Xiong W, Tan M, et al. The reverse Warburg effect is likely to be an Achilles' heel of cancer that can be exploited for cancer therapy. Oncotarget. 2017;8:57813–25.
7. Martinez-Outschoorn UE, Lin Z, Trimmer C, Flomenberg N, Wang C, Pavlides S, et al. Cancer cells metabolically "fertilize" the tumor microenvironment with hydrogen peroxide, driving the Warburg effect: implications for PET imaging of human tumors. Cell Cycle. 2011;10:2504–20.
8. Kroemer G, Marino G, Levine B. Autophagy and the integrated stress response. Mol Cell. 2010;40:280–93.
9. Kim BG, Gao MQ, Choi YP, Kang S, Park HR, Kang KS, et al. Invasive breast cancer induces laminin-332 upregulation and integrin beta4 neoexpression in myofibroblasts to confer an anoikis-resistant phenotype during tissue remodeling. Breast Cancer Res. 2012;14:R88.
10. Yang L, Hou Y, Yuan J, Tang S, Zhang H, Zhu Q, et al. Twist promotes reprogramming of glucose metabolism in breast cancer cells through PI3K/AKT and p53 signaling pathways. Oncotarget. 2015;6:25755–69.
11. Valadi H, Ekstrom K, Bossios A, Sjostrand M, Lee JJ, Lotvall JO. Exosome-mediated transfer of mRNAs and microRNAs is a novel mechanism of genetic exchange between cells. Nat Cell Biol. 2007;9:654–9.
12. Peterkofsky B, Prather W. Correlation between the rates of aerobic glycolysis and glucose transport, unrelated to neoplastic transformation, in a series of BALB 3T3-derived cell lines. Cancer Res. 1982;42:1809–16.
13. Maycotte P, Marin-Hernandez A, Goyri-Aguirre M, Anaya-Ruiz M, Reyes-Leyva J, Cortes-Hernandez P. Mitochondrial dynamics and cancer. Tumour Biol. 2017;39:1010428317698391.
14. Esteban-Martinez L, Sierra-Filardi E, McGreal RS, Salazar-Roa M, Marino G, Seco E, et al. Programmed mitophagy is essential for the glycolytic switch during cell differentiation. EMBO J. 2017;36:1688–706.
15. Kubli DA, Gustafsson AB. Mitochondria and mitophagy: the yin and yang of cell death control. Circ Res. 2012;111:1208–21.
16. Quelo I, Gauthier C, Hannigan GE, Dedhar S, St-Arnaud R. Integrin-linked kinase regulates the nuclear entry of the c-Jun coactivator alpha-NAC and its coactivation potency. J Biol Chem. 2004;279:43893–9.
17. Ke H, Harris R, Coloff JL, Jin JY, Leshin B, Miliani de Marval P, et al. The c-Jun NH2-terminal kinase 2 plays a dominant role in human epidermal neoplasia. Cancer Res. 2010;70:3080–8.
18. Novak I, Kirkin V, McEwan DG, Zhang J, Wild P, Rozenknop A, et al. Nix is a selective autophagy receptor for mitochondrial clearance. EMBO Rep. 2010;11:45–51.
19. Schwarten M, Mohrluder J, Ma P, Stoldt M, Thielmann Y, Stangler T, et al. Nix directly binds to GABARAP: a possible crosstalk between apoptosis and autophagy. Autophagy. 2009;5:690–8.
20. Roach PJ. AMPK -> ULK1 -> autophagy. Mol Cell Biol. 2011;31:3082–4.
21. Sheen JH, Zoncu R, Kim D, Sabatini DM. Defective regulation of autophagy upon leucine deprivation reveals a targetable liability of human melanoma cells in vitro and in vivo. Cancer Cell. 2011;19:613–28.
22. Liu M, Quek LE, Sultani G, Turner N. Epithelial-mesenchymal transition induction is associated with augmented glucose uptake and lactate production in pancreatic ductal adenocarcinoma. Cancer Metab. 2016;4:19.
23. Kim BG, An HJ, Kang S, Choi YP, Gao MQ, Park H, et al. Laminin-332-rich tumor microenvironment for tumor invasion in the interface zone of breast cancer. Am J Pathol. 2011;178:373–81.
24. Kim BG, Gao MQ, Kang S, Choi YP, Lee JH, Kim JE, et al. Mechanical compression induces VEGFA overexpression in breast cancer via DNMT3A-dependent miR-9 downregulation. Cell Death Dis. 2017;8:e2646.
25. Sena LA, Chandel NS. Physiological roles of mitochondrial reactive oxygen species. Mol Cell. 2012;48:158–67.
26. Jezek J, Cooper KF, Strich R. Reactive oxygen species and mitochondrial dynamics: the Yin and Yang of mitochondrial dysfunction and cancer progression. Antioxidants. 2018;7:1–24.
27. Renschler MF. The emerging role of reactive oxygen species in cancer therapy. Eur J Cancer. 2004;40:1934–40.
28. Takahashi A, Ohtani N, Yamakoshi K, Iida S, Tahara H, Nakayama K, et al. Mitogenic signalling and the p16INK4a-Rb pathway cooperate to enforce irreversible cellular senescence. Nat Cell Biol. 2006;8:1291–7.
29. Frank M, Duvezin-Caubet S, Koob S, Occhipinti A, Jagasia R, Petcherski A, et al. Mitophagy is triggered by mild oxidative stress in a mitochondrial fission dependent manner. Biochim Biophys Acta. 2012;1823:2297–310.
30. Liou GY, Storz P. Reactive oxygen species in cancer. Free Radic Res. 2010;44:479–96.
31. Li XL, Liu L, Li DD, He YP, Guo LH, Sun LP, et al. Integrin beta4 promotes cell invasion and epithelial-mesenchymal transition through the modulation of Slug expression in hepatocellular carcinoma. Sci Rep. 2017;7:1–12.
32. McKeown SR. Defining normoxia, physoxia and hypoxia in tumours-implications for treatment response. Br J Radio. 2014;87:20130676.
33. Pavlides S, Vera I, Gandara R, Sneddon S, Pestell RG, Mercier I, et al. Warburg meets autophagy: cancer-associated fibroblasts accelerate tumor growth and metastasis via oxidative stress, mitophagy, and aerobic glycolysis. Antioxid Redox Signal. 2012;16:1264–84.
34. Xiao B, Goh JY, Xiao L, Xian H, Lim KL, Liou YC. Reactive oxygen species trigger Parkin/PINK1 pathway-dependent

mitophagy by inducing mitochondrial recruitment of Parkin. J Biol Chem. 2017;292:16697–708.
35. Cicenas J, Zalyte E, Rimkus A, Dapkus D, Noreika R, Urbonavicius S. JNK, p38, ERK, and SGK1 inhibitors in cancer. Cancers. 2017;10:1–12.
36. Liu SY, Ge D, Chen LN, Zhao J, Su L, Zhang SL, et al. A small molecule induces integrin beta4 nuclear translocation and apoptosis selectively in cancer cells with high expression of integrin beta4. Oncotarget. 2016;7:16282–96.
37. Kosgodage US, Mould R, Henley AB, Nunn AV, Guy GW, Thomas EL, et al. Cannabidiol (CBD) Is a novel inhibitor for exosome and microvesicle (EMV) release in cancer. Front Pharm. 2018;9:889.
38. Messeguer X, Escudero R, Farre D, Nunez O, Martinez J, Alba MM. PROMO: detection of known transcription regulatory elements using species-tailored searches. Bioinformatics. 2002;18:333–4.
39. Vallejo AN, Pogulis RJ, Pease LR. PCR mutagenesis by overlap extension and gene SOE. CSH Protoc. 2008;2008:pdbprot4861.